# Parameters Regulating Interfacial and Mechanical Properties of Short Glass Fiber Reinforced Polypropylene

**CLAUDINE ROUX, JOHANNE DENAULT, MICHEL F. CHAMPAGNE**

Industrial Materials Institute, National Research Council Canada,
75 de Mortagne, Boucherville, Québec, J4B 6Y4, Canada

*Received 5 November 1998; accepted 11 April 1999*

**ABSTRACT:** The performance of thermoplastic composites is known to depend on the intrinsic properties of the two composite components, the quality of the fiber–matrix interface, and the crystalline properties of their matrix. The objective of this work is to characterize the effect of the addition of modified polypropylene (PP) and silane coupling agent on the mechanical and interfacial properties of short fiber reinforced PP composites. Differential scanning calorimetry (DSC), single fiber composite fragmentation tests (SFC), and mechanical testing are used to understand the different parameters regulating the interfacial properties of composites. No influence of the modified PP on the level of crystallinity is observed. Some differences in the size of the spherulites are observed for acrylic acid grafted PP (PP-*g*-AA). Those samples also show lower mechanical properties in spite of good interfacial interactions. Maleic anhydride grafted PP (PP-*g*-MAh) leads to better mechanical performances than PP-*g*-AA. A high MAh content PP-*g*-MAh grade with low viscosity is the best polymeric additive used in the present work. © 2000 John Wiley & Sons, Inc. J Appl Polym Sci 78: 2047–2060, 2000

**Key words:** interfacial interactions; single fiber composite fragmentation test; grafting level; glass fibers; polypropylene

## INTRODUCTION

For numerous reasons, thermoplastic resins are gradually replacing thermoset matrices in the development of new composites. Unlike their thermoset counterpart, thermoplastics are water resistant, reshapable, and recyclable and their processing does not generate any volatile organic contaminant (VOC); these are all very important properties in the environmentally friendly era that has begun in the past decade. They also exhibit short process cycle times, increased toughness, and impact resistance compared to thermoset resins. Polypropylene (PP) is extensively used in the composite industry because it is an inexpensive material that shows good mechanical performance combined with excellent chemical and weather resistance.

Many studies have been conducted on composites of PP and different types of reinforcement such as carbon fibers,[1–3] glass fibers,[4–7] polymeric fibers,[1,2] or mica.[8] Most of them relate the mechanical properties to the filler concentration, size, and dispersion and to the PP morphology. PP exhibits different types of crystallinities, and their influence on the interfacial interactions between the filler and matrix has been extensively studied.[1–4,9,10] It is also well known that the mechanical performance of composites is closely related to the interfacial cohesion present between the matrix and the filler. The efficiency of the filler in reinforcing the polymeric matrix depends

*Correspondence to:* C. Roux.

Journal of Applied Polymer Science, Vol. 78, 2047–2060 (2000)

on its mechanical properties, level of shape anisotropy, alignment with respect to the testing directions, and, ultimately, the interfacial strength of the system. The latter factor is especially important because the usefulness of any given filler would be severely reduced if there were a lack of adhesion between the two components of the composite. Whenever the composite is subjected to a mechanical stress, the adhesion between the reinforcing filler and the surrounding matrix is responsible for the stress transfer from the matrix to the filler.

Interactions between glass and PP are extremely limited because glass has a polar surface and PP is a nonpolar polyolefin. A way to promote the adhesion between them is to modify the surface of the glass fibers with an appropriate sizing. The addition of a chemically modified PP can also lead to the creation of a better interface. Functionalized PPs such as acrylic acid grafted PP (PP-*g*-AA)[11,12] and maleic anhydride grafted PP (PP-*g*-MAh)[13,14] are commercially available and are used together with suitably sized glass fibers to improve the tensile strength of the composites.

Short glass fiber reinforced PP composites have already been investigated on the basis of fiber length and orientation.[15] The injection molding conditions together with the sizing and PP matrix composition have also been studied in terms of their influence on the fiber length and distribution[15–17] and their mechanical behavior.[18,19] The objective of this work is to characterize the effect of the addition of grafted PP and silane coupling agent on the tensile and impact properties and to relate the performance to the interfacial strength of the PP composites. The method chosen to evaluate the interfacial properties of the different systems is the fragmentation test. Much work has been done on the characterization of thermoset-based single fiber composites (SFCs) using the fragmentation test.[20–23] Although some work has been done on thermoplastic systems,[24,25] the interfacial characterization of PP SFC has not been characterized as extensively.[26]

Measurement of interfacial characteristics in composites can be performed through the SFC techniques. Different SFC techniques have been developed to characterize the strength at the interface between the fiber and the matrix, which is the interfacial shear strength (IFSS). The IFSS is an evaluation of the efficiency of the interface to transfer the applied stress from the matrix to the fiber before decohesion occurs. Microindentation, SFC microbond, and fragmentation tests[27,28] are among the other methods that are recognized to measure the level of adhesion between the matrix and the fiber.

The choice of an appropriate sizing is based on the physical and chemical interactions that are possibly generated between the fiber sizing and the surrounding matrix. The chemistry involved in the compatibilization of a PP/polyamide (PP/PA) blend using PP-*g*-MAh as the interfacial modifier has inspired the choice of a sizing. The creation of a copolymer PP/PA by the reaction of the MAh functionalities of PP-*g*-MAh with the amine groups of PA was reported and proved to be a key factor in the compatibilization of such an immiscible blend.[29] One of the sizings considered in this work is the $\gamma$-aminopropyl-triethoxysilane ($\gamma$-APS). The secondary amine group is expected to react with the MA and AA functionalities borne by the modified PP.

AA and MAh grafted PP with different grafting levels and molecular weights were added to glass fibers/PP composites prepared from fibers treated with two different sizings. The influence of the modified PPs and fiber sizings on the crystallinity of the systems was investigated; the crystallization behavior was studied using differential scanning calorimetry (DSC). Composites of commercial fibers sized for thermoplastics sized fibers (TSFs), pyrolyzed fibers (PFs), and pyrolyzed/sized fibers (PSFs) were studied in terms of their interfacial properties: fragmentation tests were performed on SFCs using the different grafted PP resins as adhesion promoters. The study of the influence of grafted PP and the different fiber sizings on the mechanical properties of the composites contributes to the understanding of the different parameters regulating the strength of the interface.

## EXPERIMENTAL

### Materials

Some of the characteristics of the resins used for sample preparation are summarized in Table I. Functionalized resins were dried at 70°C under a dynamic vacuum for 12 h prior to use. The short fibers ($\sim$ 4.7 mm) sized for thermoplastic resins were supplied by Vetrotex Certainteed (XA4 J96 P201). Three series of short fiber composites were extruded. In the first series fibers sized for thermoplastic resins were used as received and compounded in different amounts (0, 20, 25, 35 wt %)

**Table I Selected Characteristics of Polypropylene and Modified Polypropylenes**

| Acronym | Functionality | Melt Flow Index[a] (g/10 min) | Supplier Grade |
|---|---|---|---|
| PP | None | 5 | Montell PV314 |
| PP-*g*-MAh | Maleic anhydride | 5 | Uniroyal PolyBond 3001 |
| PP-*g*-MAl | Maleic anhydride | 50 | Uniroyal PolyBond 3150 |
| PP-*g*-AA | Acrylic acid | 40 | Uniroyal PolyBond 1001 |

[a] The data were taken from Montell and Uniroyal data sheets.

with different percentages of grafted PP (0, 2, 5, 10, 15 wt %). In the second series of experiments the fibers were pyrolyzed at 500°C for 12 h. Half were compounded with PP at 20 wt % and different amounts of grafted PP (0, 2, 5, 10, 15 wt %). The grafting level of PP-*g*-AA, PP-*g*-MAh, and PP-*g*-MAl were approximately 6, 0.15, and 0.8%,[30] respectively. Finally, the second half of the pyrolyzed fibers was sized using γ-APS (A-1100, Union Carbide Chemicals and Plastics) and compounded with PP and grafted PP at the same ratios.

The coating of the pyrolyzed fibers was done using the following procedure. An aqueous solution of 0.25 wt % of silane coupling agent was prepared in acidified water using formic acid as the acidifier to lower the pH to 4. According to the supplier directions, 10 g of γ-APS were used per kilogram of fibers. The acidification of the water was done prior to the addition of silane to the solution. The fibers were immersed in the silane solution for 1 h and then filtered and heated under a vacuum at 70°C for about 12 h. Long fibers used for the preparation of SFCs that had the same thermoplastic sizing as the short fibers were also pyrolyzed and sized using the same procedure.

The composites were prepared in a 30-mm Werner–Pfleiderer twin-screw extruder ($L/D = 33$). In order to minimize fiber length attrition, the fibers were added through a venting port in the second half of the extruder and from there only conveying elements were used. The composites were compounded at 210°C, 150 rpm, and a throughput rate of 6 kg/h.

## Characterization

The crystallinity characterization was performed on samples from injection molded specimens of about 10 mg using a Perkin Elmer DSC-7 apparatus; all experiments were conducted under a nitrogen atmosphere. The heating and cooling rates were set at 20°C/min.

Scanning electron microscopy (SEM) observations were performed on a Jeol JSM-T220 microscope. The surfaces of the fractured samples were Au/Pd sputtered for qualitative evidence of fiber–matrix adhesion. The crystalline morphology of the PP matrix was also observed using SEM. The samples were first embedded in epoxy resin and polished. They were then etched in a solution of sulfuric acid, *ortho*-phosphoric acid, and potassium permanganate during 30 min. The samples and the etching solution were then poured in a solution of sulfuric acid and demineralized water (2 : 7). Samples were successively washed using hydrogen peroxide (30%), demineralized water, and acetone. A very thin Au/Pd coating was sputtered in order to leave the exposed crystalline structure as clear as possible.

The fragmentation test was used in comparing the relative interfacial interactions between the different matrix–fiber combinations investigated. Thin sheets of PP containing 0 or 5% modified PP were prepared by compression molding under a vacuum from pellets of twin-screw extruded PP/grafted PP compounds. Two preshaped dogbones (ASTM type 1) were cut from those sheets; a long fiber was glued with two small epoxy glue droplets near the extremities of one of the dogbones. SFCs were compression molded at 210°C during 5 min at a pressure of 100 psi. The specimens were tested under tensile load parallel to the fiber axis (Fig. 1) at 23°C and 50% relative humidity. Tests were performed at a crosshead speed of 0.5 mm/min up to 7% strain, which is well above the elongation at break of glass fibers (~ 2%). We considered that such a level of strain is sufficient to break the fiber to its critical length ($l_c$) before the fiber debonds from the matrix. The fragment

lengths were measured using a stereomicroscope. A minimum of 60 fragments was measured in evaluating the $l_c$ value of each composite system investigated.

Tensile testing was done following the ASTM D-638 procedure using ASTM type 1 3 mm thick specimens prepared with an 80-ton injection molding machine. The temperature of the melt was set in the range of 210–225°C, the mold temperature was 50°C, and the screw rotation speed was 250 rpm. Testing was performed at 23°C and 50% relative humidity at a crosshead speed of 10 mm/min using an Instron tensile tester (model 1123) equipped with extensometers. Charpy impact tests were performed on 3 mm thick notched bars following the ASTM D-256 procedure.

## RESULTS AND DISCUSSION

### Crystallinity and Crystalline Morphology

The thermal history of thermoplastic composites is a very important factor, considering the influence of crystallinity on their properties.[31] PP is a semicrystalline polymer, and its properties are influenced by its crystalline structure and content. The crystalline phase can vary in terms of spherulite number, size, and perfection, depending on the conditions under which the specimens are formed. Injection molding of thermoplastic composites involves a nonisothermal history. In order to investigate the effect of the addition of grafted PP on the crystallization behavior of a PP matrix composite, the thermal conditions of the injection molding process were tentatively simulated by DSC. Under a nitrogen atmosphere the short fiber composites were heated from room temperature to 210°C at a heating rate of 20°C/min. After 5 min at 210°C the samples were cooled to room temperature at a cooling rate of 20°C/min. During the cooling process the crystallization exotherms were recorded and analyzed in terms of the temperature of crystallization onset, $T_{co}$, the maximum temperature of crystallization peak, $T_{cp}$, the temperature corresponding to the end of the crystallization process, $T_{ce}$, and the crystallization enthalpy, $\Delta H_c$ (Fig. 2). For comparison purposes, the crystallization behavior of the unreinforced resins systems was also analyzed.

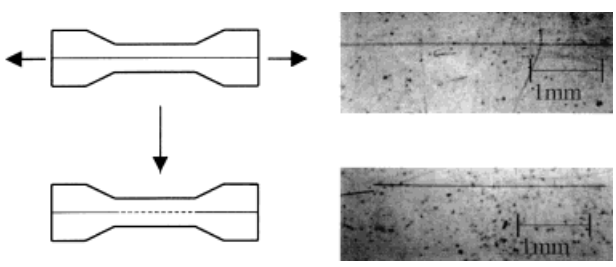


**Figure 1** Schematic representation of the single fiber composite method.

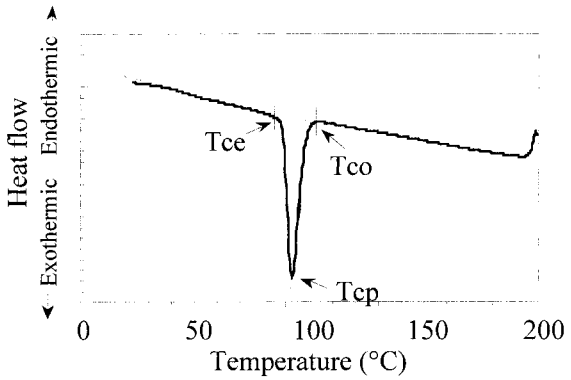


**Figure 2** Typical DSC curve of a PP sample and definition of crystallization parameters.

The enthalpy of fusion of all samples (unreinforced matrix or composites) were calculated from the DSC thermograms, and no significant difference was observed between them. Table II presents the crystallization data obtained for the unreinforced resins.

From these results it can be observed that the addition of grafted PP to pure PP resin affects the crystallization behavior of the matrix. The $T_{co}$ and $T_{cp}$ increased for all samples containing grafted PP, indicating that such additives have some nucleating properties. The increase of $T_{co}$ is related to an improved nucleation process occurring sooner during cooling. The $T_{cp}$ parameter represents the change from the fast primary crystallization mechanism to the slow secondary crystallization mechanism.[32] The change arises from the impingement of the spherulite crystalline structures. The primary crystallization is a fast process (growth of the spherulites) because prior to impingement all of the spherulites grow in the amorphous polymer without restriction. After complete impingement secondary crystallization can only proceed in the interlamellar regions and consequently proceeds at a slower rate. The samples containing PP-*g*-AA showed the highest increase in $T_{co}$, indicating higher nucleating ability compared to maleated PP. Still, for PP-*g*-AA samples the $T_{co}$–$T_{cp}$ parameter is constant no matter

**Table II Crystallization Behavior of Pure PP and Blends of PP Grafted/PP**

| Materials | $T_{co}$ (°C) | $T_{cp}$ (°C) | $T_{ce}$ (°C) | $T_{co}$–$T_{cp}$ (°C) | $T_{cp}$–$T_{ce}$ (°C) |
|---|---|---|---|---|---|
| Pure PP | 115 | 106 | 95 | 9 | 11 |
| PP-*g*-AA | | | | | |
| 2% | 121 | 112 | 100 | 9 | 12 |
| 5% | 121 | 112 | 97 | 9 | 15 |
| 10% | 124 | 115 | 100 | 9 | 15 |
| 15% | 125 | 116 | 101 | 9 | 15 |
| PP-*g*-MAl | | | | | |
| 2% | 118 | 107 | 96 | 11 | 11 |
| 5% | 117 | 105 | 93 | 12 | 12 |
| 10% | 118 | 106 | 95 | 12 | 11 |
| 15% | 118 | 106 | 96 | 12 | 12 |
| PP-*g*-MAh | | | | | |
| 2% | 118 | 108 | 97 | 10 | 11 |
| 5% | 120 | 110 | 98 | 10 | 12 |
| 10% | 118 | 110 | 99 | 8 | 11 |
| 15% | 117 | 106 | 96 | 11 | 10 |

the amount of grafted PP and it also shows an unchanged temperature interval for primary crystallization compared to pure PP. The increase in the $T_{cp}$–$T_{ce}$ parameter suggests a longer period of time allowed for secondary crystallization. The primary crystallization occurs in a slightly larger temperature interval ($T_{co}$–$T_{cp}$ = 10–12°C) for samples containing PP-*g*-MAh, which shows the longer time required for nucleation and spherulite growth. The secondary crystallization remains identical to that of pure PP and is not influenced by PP-*g*-MAh concentrations.

Complementary to the DSC crystallization analysis, chemical etching and observation from SEM revealed the crystalline morphology of the matrix in the composites. Figure 3 shows that the

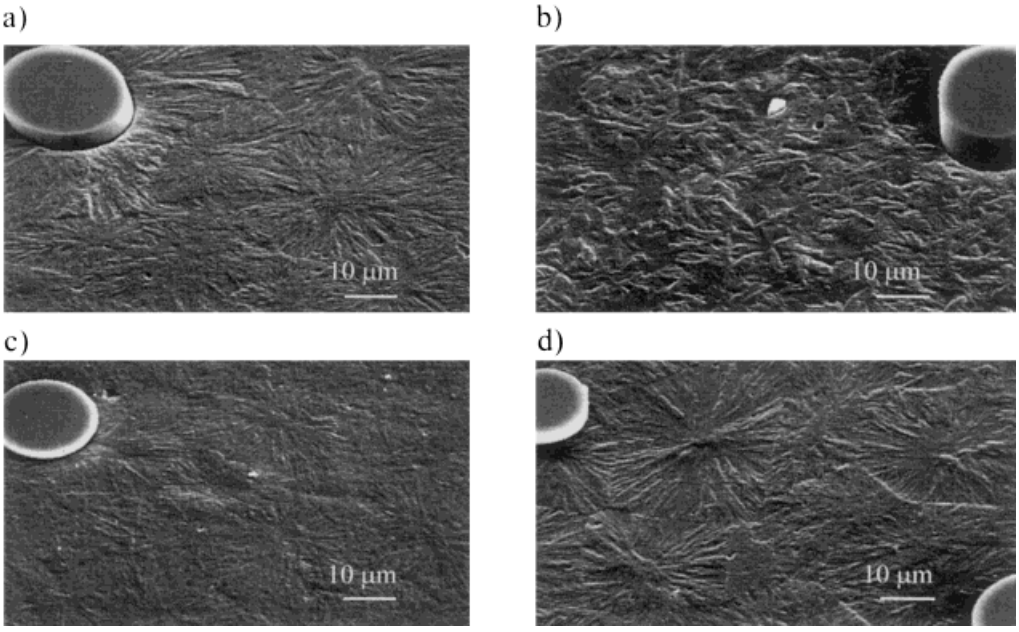


**Figure 3** SEM micrographs of etched surfaces of 25 wt % glass fiber/PP composites containing (a) pure PP, (b) 15% PP-*g*-AA, (c) 15% PP-*g*-MAh, and (d) 15% PP-*g*-MAl (original magnification ×2000).

**Table III Crystallization Behavior of Short Glass Fiber/PP Composites**

| Materials | $T_{co}$ (°C) | $T_{cp}$ (°C) | $T_{ce}$ (°C) | $T_{co}$–$T_{cp}$ (°C) | $T_{cp}$–$T_{ce}$ (°C) |
|---|---|---|---|---|---|
| Pure PP | | | | | |
| TSF | 115 | 106 | 95 | 9 | 11 |
| PP | 121 | 111 | 101 | 10 | 10 |
| 15% PP-*g*-AA | 125 | 116 | 101 | 9 | 15 |
| 15% PP-*g*-MAl | 123 | 112 | 103 | 11 | 9 |
| 15% PP-*g*-MAh | | | | | |
| PF | 123 | 112 | 102 | 11 | 10 |
| PP | 118 | 108 | 98 | 10 | 10 |
| 15% PP-*g*-AA | 124 | 114 | 100 | 10 | 14 |
| 15% PP-*g*-MAl | 120 | 110 | 97 | 10 | 13 |
| 15% PP-*g*-MAh | | | | | |
| PSF | 120 | 110 | 100 | 10 | 10 |
| PP | 120 | 109 | 98 | 11 | 11 |
| 15% PP-*g*-AA | 125 | 116 | 102 | 9 | 14 |
| 15% PP-*g*-MAl | 120 | 109 | 98 | 11 | 11 |
| 15% PP-*g*-MAh | 119 | 110 | 99 | 9 | 11 |

TSF, thermoplastic sized fibers; PF, pyrolyzed fibers; PSF, pyrolyzed/A-1100 sized fibers.

crystalline structure of the pure PP matrix [Fig. 3(a)] is well modified by the addition of PP-*g*-AA [Fig. 3(b)]. In this case the matrix microstructure is characterized by less well-defined, more numerous, and smaller crystalline entities. This is consistent with the higher $T_{co}$ observed. In the PP-*g*-MAh sample the effect was much less marked: a slight modification of the crystalline structure is suggested in Figure 3(c) that could relate to the higher $T_{co}$–$T_{cp}$ parameter. Finally, the PP-*g*-MAl sample microstructure seems to be equivalent to that of the pure PP matrix [Fig. 3(d)].

The results of the crystallization analysis of the different short glass fiber/PP composites are presented in Table III. The results show that the addition of glass fibers to pure PP increases the $T_{co}$, $T_{cp}$, and $T_{ce}$ parameters and this effect is slightly less important for composites made from pyrolyzed fibers. These results indicate that glass fibers could act as nucleating agent for the PP matrix. However, optical microscopy observations of the crystallization process do not allow the detection of any specific crystallization at the fiber surface. In fact, for all three types of glass fiber composites, crystallization began in the bulk of the PP matrix. The higher values of $T_{co}$ and $T_{cp}$ could only partially be attributed to the presence of glass fragments, which can act as nucleation sites for the PP matrix. The $T_{co}$–$T_{cp}$ and $T_{cp}$–$T_{ce}$ parameters are almost constant for all types of fibers, indicating that the type of fibers present does not influence the primary and secondary crystallization rates.

The comparison of DSC data for samples of unreinforced and reinforced PP-*g*-AA/PP matrix also shows that the presence of the glass fibers slightly affects the crystallization process of the matrix. All crystallization temperature are almost constant compared to that of unreinforced resins with the exception for composites containing pyrolyzed fibers. In that case a small decrease in the crystallization temperature parameters is noticed. As already observed for unreinforced samples, all crystallization temperatures are higher for PP-*g*-AA samples than for composites containing maleated PP. This would tend to prove that the matrix mainly drives the nucleation of PP-*g*-AA/PP itself. The secondary crystallization, characterized by $T_{cp}$–$T_{ce}$, occurs systematically in a larger range of temperatures (14–15°C) for all three types of fibers. The higher number of smaller spherulites may explain the increase in the $T_{cp}$–$T_{ce}$ parameter.

The properties of reinforced PP-*g*-MAl/PP and PP-*g*-MAh/PP samples show some differences compared to the unreinforced ones. The $T_{co}$, $T_{cp}$, and $T_{ce}$ increased with the presence of fibers, indicating some nucleating effect of the fibers. In the PP-*g*-MAl, the $T_{co}$–$T_{cp}$ and $T_{cp}$–$T_{ce}$ parameters decrease: the primary and secondary crystallizations are shortened, except for the composites containing pyrolyzed fibers where the secondary crystallization is slightly longer. This suggests that the crystallization process is more rapid, because no significant change in the $\Delta H_c$ was observed. The $T_{co}$–$T_{cp}$ and $T_{cp}$–$T_{ce}$ parameters re-

**Table IV Fragmentation Test Data: Critical Fiber Length ($l_c$) Obtained for SFCs of Different Fiber Sizing and Different Grafted PPs (5% Grafted PP in 95% Pure PP) as Adhesion Promoters**

| Matrix | Thermoplastic Sizing $l_c$ (mm) | Pyrolyzed Fibers $l_c$ (mm) | Pyrolyzed/A-1100 $l_c$ (mm) |
|---|---|---|---|
| Pure PP | 5.1 | 4.4 | 5.5 |
| 5% PP-*g*-AA | 2.6 | 2.7 | 2.1 |
| 5% PP-*g*-MAl | 2.2 | 2.2 | 1.8 |
| 5% PP-*g*-MAh | 4.4 | 3.5 | 2.2 |

main almost identical for PP-*g*-MAh. The overall crystallization process is shifted toward higher temperatures, but the primary and secondary crystallizations still occur in the same 10–11°C interval. The main change seems to be related to the nucleation process that occurs at a higher temperature for reinforced samples compared to unreinforced ones.

To summarize, the addition of grafted PP to unreinforced PP samples increases the $T_{co}$, $T_{cp}$, and $T_{ce}$. The addition of fibers also increases those parameters for all types of fibers. Also, the $T_{co}$–$T_{cp}$ parameter related to primary crystallization is almost constant for reinforced and unreinforced samples containing PP-*g*-AA. That parameter slightly decreases for composites containing maleated PP compared to unreinforced ones. The $T_{cp}$–$T_{ce}$ parameter remains almost unchanged for all samples, being maximal for samples containing PP-*g*-AA. That increase in the interval of temperature allows a longer time for secondary crystallization.

## Interfacial Characterization

One of the simplest ways to achieve interfacial characterization is the SFC fragmentation test. This test consists of applying a continuous tensile stress to the SFC specimen. The applied stress will induce fiber breaking when the tensile stress of the fiber, $\sigma_f$, at a given initial length is reached. As the test goes on, the fiber fragments get shorter, down to a length equivalent to the critical fiber length, $l_c$, for a given system. At this point no more fiber breaking occurs and the shear stress along the fiber is considered to be constant. According to the model of Kelly and Tyson,[24] the following equation shows the linear relation between $l_c$ and the interfacial shear strength $\tau$:

$$\tau = \frac{d\sigma_f(l_c)}{2l_c}$$

where $d$ is the diameter of the fiber and $\sigma_f(l_c)$ is the fiber tensile strength at its critical length. A higher $\tau$ and therefore a smaller $l_c$ characterize a better interface. The $\sigma_f(l_c)$ was not determined here and the relative strength of the composite interface is compared using the critical fiber length. Therefore, no comparisons between the SFC of different fibers are considered and only the SFC of an identical fiber are compared using their $l_c$ parameter.

The $l_c$ parameter can be calculated using the average length of the fragments, $\bar{l}$, which is determined by the $d_{50}$ of the cumulative distribution of the fiber fragment length. Because $\bar{l}$ is expected to have a value between $\frac{1}{2}l_c$ and $l_c$, the following approximation will be used[24]:

$$l_c = \frac{4\bar{l}}{3}$$

Table IV summarizes the data obtained for the fragmentation test of SFCs containing the three different types of fibers: TSFs, PFs, and pyrolyzed/γ-APS sized fibers. The same three grafted PPs were tested as adhesion promoters.

For each type of fiber the results show that the addition of grafted PP promotes adhesion between the matrix and the fiber. The enhancement is particularly important in the case of matrices containing PP-*g*-AA and PP-*g*-MAl. For these matrices the $l_c$ parameter is decreased by a factor of 2 compared to the SFC of pure PP. A first series of experiments had already been performed on SFCs containing either pure PP matrix or 15% of both grafted PP in 85% PP and a fiber treated with proprietary thermoplastic resins sizing (TSF). These results from a previous work are reported in ref. 27. The same order of efficiency between the different grafted PPs was observed. Looking at the results obtained for SFCs with TSFs, the average error on $l_c$ is circa 48%. As already men-

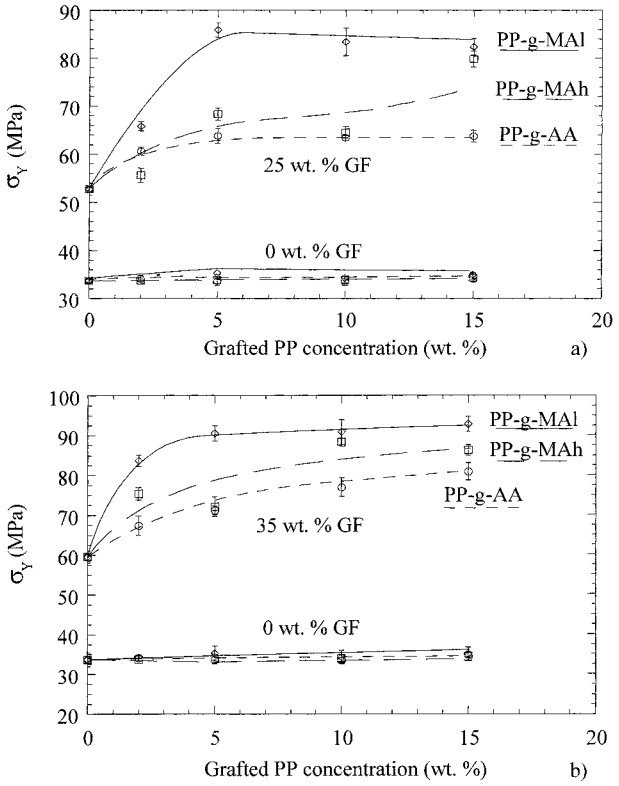


**Figure 4** Effect of grafted PP concentration on the strength at yield of glass fiber/PP composites containing (a) 25 wt % or (b) 35 wt % glass fibers coated with a thermoplastic sizing.

tioned, the critical fiber lengths obtained show a clear improvement of the SFC interface using PP-*g*-AA and PP-*g*-MAl. In the PP-*g*-MAh no obvious enhancement of the SFC interface can be concluded from the $l_c$ value obtained.

The results of the fragmentation tests on the SFCs with PF and PSF sized fibers show the efficiency of the γ-APS sizing for the improvement of the fiber to matrix adhesion. All values of $l_c$ decreased compared to pyrolyzed fibers SFCs. The average error on $l_c$ for both types of fibers was 32%. The $l_c$ value obtained for the SFCs of pyrolyzed fibers decreased substantially for SFCs containing PP-*g*-AA and PP-*g*-MAl compared to pure PP.

## Mechanical Properties

Figures 4–7 show the results of the mechanical characterization obtained for composites made from fibers coated with a thermoplastic sizing. Figure 4 shows the effect of grafted resins on the yield stress, $\sigma_Y$, for samples containing 25 and 35

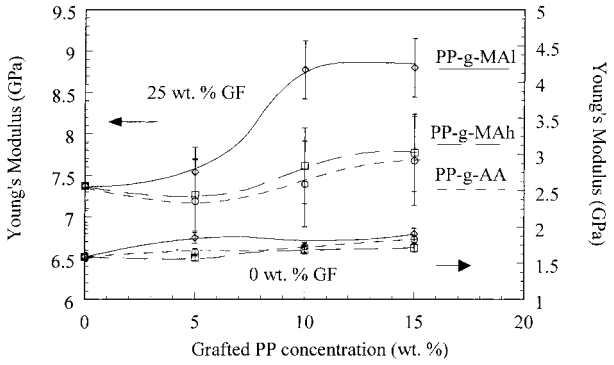


**Figure 5** Effect of grafted PP concentration on the Young's modulus of 25 wt % glass fiber/PP composites (thermoplastic sizing).

wt % glass fibers. The stress–strain curves of each of the composites showed brittle fractures. The tensile properties of TSF/pure PP composites were considerably improved by the addition of grafted resins. For composites containing 25 wt % glass fiber the yield stress increased 20 (PP-*g*-AA), 50 (PP-*g*-MAh), and 55% (PP-*g*-MAl) over the nonmodified systems. The addition of grafted PP to samples containing 35 wt % glass fibers produced similar improvements: a 35–55% increase of the $\sigma_Y$ value was obtained. At both glass fiber contents investigated, the yield stress increased at a grafted resins content as low as 5%, which is even optimum in the composites containing PP-*g*-MAl. The strength of the different matrices without fibers is shown in the lower part of the graphs. The contribution of the grafted PP to the matrix tensile properties seems to be relatively limited, according to the very small changes observed in their yield stress (ductile fractures).

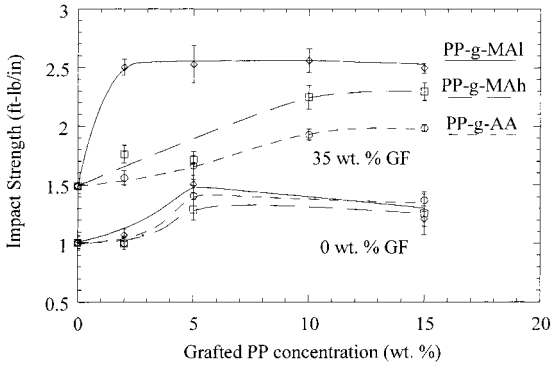


**Figure 6** Effect of grafted PP concentration on the impact strength of glass fiber/PP composites (thermoplastic sizing).

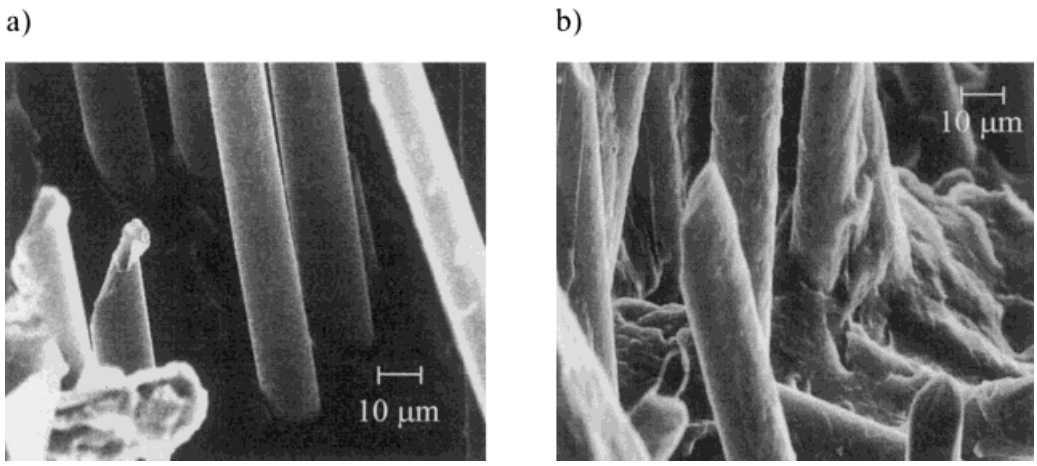


**Figure 7** SEM micrographs of ruptured surfaces of 25 wt % glass fiber composites.

The influence of grafted PP on the composites' Young's modulus, $E$, is illustrated in Figure 5. The pure PP reinforced sample showed a net increase in their modulus ($E$ = 7.4 GPa) compared to the unreinforced one (1.5 GPa). Taking into account the error associated with the measurement of $E$, slight increases are observed for composites containing PP-*g*-AA ($E$ = 7.7 GPa) and PP-*g*-MAh ($E$ = 7.8 GPa). The significant augmentation up to 8.8 GPa of the modulus of composites containing PP-*g*-MAl demonstrates the higher efficiency of that grafted PP in enhancing the modulus of the composites compared to the two other coupling agents. Because the Young's modulus of matrices (without GF) is not significantly influenced by the presence of grafted PP (bottom, Fig. 5), the enhancements observed for the composites are mainly related to a better interface originating from the interaction of the grafted PP and the glass fiber surface.

The impact resistance of the samples was also characterized and is plotted against the grafted PP concentration for 0 and 35 wt % TSF content (Fig. 6). The improvement of impact resistance brought by the addition of grafted resins varies between 30 and 70% for the 35 wt % TSF composites. The impact resistance of unreinforced matrices of different compositions shows an increase of 20–30% over pure PP. The contribution of grafted PP to the impact resistance of the composite matrix appears more important than for the tensile properties.

Interestingly, in many cases a plateau value was reached at a low content ($\sim$ 5%) of grafted PP for both the tensile strength and impact resistance. The efficiency of the coupling agent investigated was found to increase as follows: PP-*g*-AA, PP-*g*-MAh, and PP-*g*-MAl. The higher reactivity of MAh is most probably related to the better performances observed for samples containing maleated PP compared to PP-*g*-AA. The higher grafting level of PP-*g*-MAl can explain the improved enhancement compared to PP-*g*-MAh. The lower viscosity of the PP-*g*-MAl may also improve the ease with which the adhesion promoter reaches the interface.

As observed in Figures 4 and 5, the influence of grafted PP on the tensile mechanical properties of the unreinforced samples is very limited. However, their impact resistance (Fig. 6) is modified by the grafted PP. The DSC data showed that the secondary crystallization was enhanced for all samples, particularly those containing PP-*g*-AA. It seems that the presence of many small spherulites has a deeper influence on the impact performance than on the tensile properties, particularly in the case of the PP-*g*-AA samples. On the other hand, the clear improvement in the tensile and impact properties is probably mostly generated by the enhanced interfacial interactions between the glass fibers and grafted PP.

The SEM micrographs of the fracture surfaces of 25 wt % TSF/PP composites containing either pure PP or 15% PP-*g*-MAl are shown in Figure 7 and provide qualitative information on the composite interface. The amount of material remaining on the fiber after tensile testing is a good indication of the interface strength. The SEM micrograph of glass fiber/pure PP composite shows clean fibers with almost no remaining matrix on the fiber surfaces. In contrast, a large amount of matrix still adheres to the fibers after fracture of

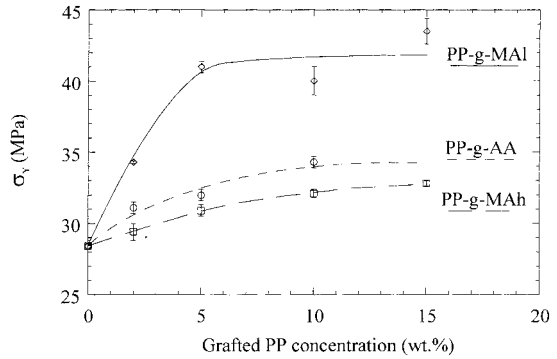


**Figure 8** Effect of grafted PP concentration on the strength at yield of 20 wt % pyrolyzed glass fiber/PP composites.

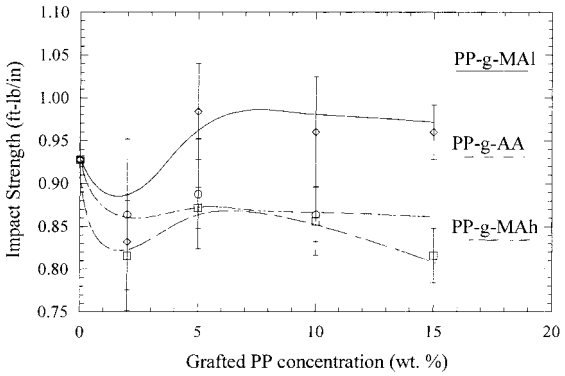


**Figure 10** Effect of grafted PP concentration on the impact strength of 20 wt % pyrolyzed glass fiber/PP composites.

the samples containing PP-*g*-MAl, which is evidence of the better fiber–matrix adhesion. No appreciable difference was noticed among the composites made from the three grafted PPs.

Figures 8–11 show the results obtained for PF and PSF composites. Figure 8 shows the influence of the grafted PP on the yield stress of composites containing 20 wt % pyrolyzed glass fibers. The $\sigma_Y$ improvement varies from 15 to 55%, depending on the nature and amounts of grafted PP added. Composites containing PP-*g*-AA and PP-*g*-MAh mainly show ductile fractures, and it is interesting to note that the addition of PP-*g*-AA results in slightly better performance than the addition of PP-*g*-MAh. The higher level of grafting of PP-*g*-AA may result in an increased number of glass/PP-*g*-AA reaction sites, even if the MAh moiety would be more reactive. The higher viscosity of PP-*g*-MAh may also prevent it from reaching the interface as easily. As observed for the TSF composites, PP-*g*-MAl is still the most efficient interface modifier even at a relatively low content ($\sim$ 5%). The low grafting level of PP-*g*-MAl (0.8%) shows the higher reactivity of MAh compared to AA. Brittle fractures are observed for samples containing PP-*g*-MAl and PF.

The aim of coating the fibers with γ-APS is to enhance the adhesion between the fiber and matrix through the reaction of the amine group of the sizing agent with the functionalities of the modified PP.[29] This strategy allows the close following of the evolution of the fiber–matrix interface and its influence on the mechanical properties of the resulting samples. The influence of the grafted PP resins on the yield stress of the composites containing pyrolyzed/γ-APS sized glass fibers is shown in Figure 9. By comparing Figures 8 and 9, the net increase in the yield stress compared to that of unsized fiber composites suggests that the interface was efficiently modified. Compared to the initial value for γ-APS sized fibers/

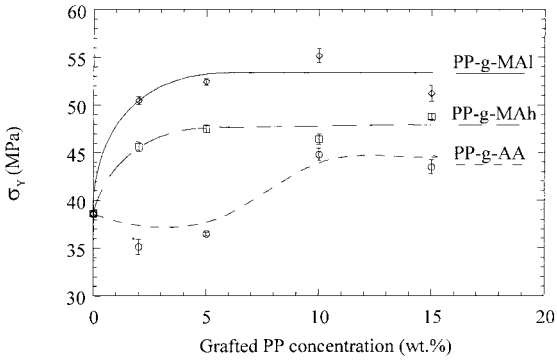


**Figure 9** Effect of grafted PP concentration on the strength at yield of 20 wt % pyrolyzed/γ-APS sized glass fiber/PP composites.

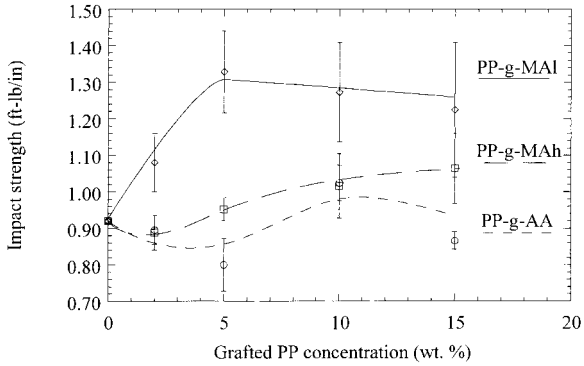


**Figure 11** Effect of grafted PP concentration on the impact strength of 20 wt % pyrolyzed/γ-APS sized glass fiber/PP composites.

pure PP, the enhancement of $\sigma_Y$ varies from 15 to 35%. The same order of increasing efficiency of the grafted resins that was obtained earlier was found: PP-*g*-AA, PP-*g*-MAh, and PP-*g*-MAl. Almost all samples showed brittle fractures.

The impact strength of pyrolyzed fiber composites (Fig. 10) did not evidence any improvement generated from the addition of grafted PP. The addition of PP-*g*-MAl produced a very small and nonsignificant increase on the order of circa 5%. In the PP-*g*-MAh and PP-*g*-AA both resins exhibited almost deleterious effects; PP-*g*-MAh gave the worst results. However, in the γ-APS sized fibers (Fig. 11) the addition of PP-*g*-MAl increased the impact resistance by 35%. PP-*g*-MAh was less effective but still increased the impact resistance of the samples by 15%. PP-*g*-AA did not bring any improvement to the impact resistance of these composites compared to unsized fiber composites.

Scanning electron micrographs of ruptured surfaces are shown on Figure 12. Figure 12(a,c,e,g) presents composites made from PFs and containing pure PP, 15% PP-*g*-AA, 15% PP-*g*-MAh, and 15% PP-*g*-MAl, respectively. They all show very similar, clean fiber surfaces, except for composites containing PP-*g*-MAl [Fig. 12(g)]. Clean fibers indicate poor interfacial interactions, a result already expected from the low mechanical properties of the pyrolyzed glass fiber composites. A plastic deformation of the matrix is noted in Figure 12(c,e), which correlate the ductile fracture and the low interfacial strength. In the composites containing PP-*g*-MAl an important amount of matrix remains on the fibers. A better interface was already suggested by the higher mechanical properties of those composites, and fragile ruptures were observed.

The micrographs in Figure 12 also show the fracture surface of composites made of pyrolyzed/γ-APS sized fibers with pure PP, 15% PP-*g*-AA, 15% PP-*g*-MAl, and 15% PP-*g*-MAl. The enhancement of the interface strength generated by combining the silane coupling agent to modified PP is clear. Effective chemical interactions were also suggested by the better mechanical properties obtained in using silane sized fibers instead of PFs for creating interface modified composites. In the pure PP composite [Fig. 12(b)] a few spots of remaining matrix appear sporadically on the fiber surface and enhanced mechanical properties are observed compared to PF/PP samples. Such results indicate some level of interactions between the γ-APS sizing of fiber and the PP matrix. Although no chemical reactions are possible, some

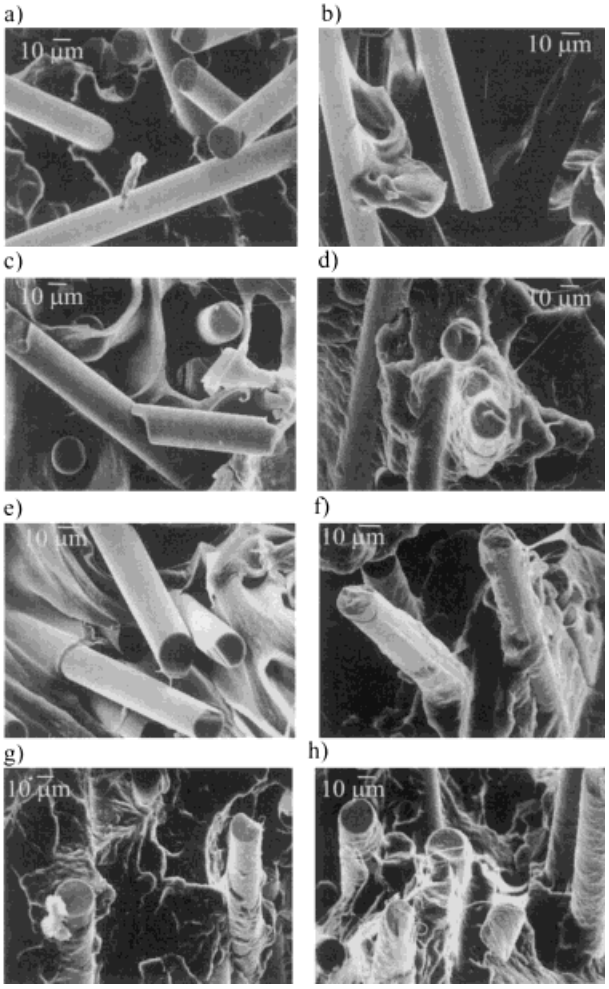


**Figure 12** SEM of fractured surfaces of 20 wt % glass fiber/PP specimens ruptured by tensile testing (original magnification ×1000).

physical interactions have to be considered. The coating of fibers with γ-APS changes the polarity and therefore the surface tension of the fibers. This might be explained by the presence of the multiple $CH_2$ groups of the γ-APS. Compared to the SiOH groups at the surface of the PFs, the $CH_2$ groups are less polar and could be partly responsible for the better affinity between the PP matrix and the glass fibers. Enhanced physical interactions result in better mechanical properties observed for the PSF/pure PP composites. Figure 12(d,f,h) shows an important increase of the amount of remaining material on the fibers. Figure 12(g,h) evidences the higher efficiency of the PP-*g*-MAl.

It is interesting to note that composites characterized by higher tensile strength show brittle fractures. For almost all PF composites, the frac-

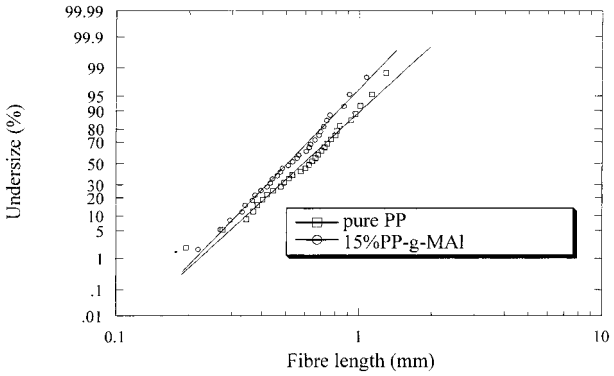


**Figure 13** Cumulative fiber length distribution for 25 wt % TSF/PP composites.

ture is ductile and can be explained by the plastic deformation of the matrix after interphase breaking (debonding) and fiber–matrix slippage have occurred. The scanning electron micrographs support this idea because the fibers on fractured surfaces are clean [Fig. 12(a,c,e)], except in the PP-*g*-MAl composites [Fig. 12(g)], which show brittle fracture. For PSF composites no plastic deformation is observed and the fracture behaviors and surfaces are those of brittle materials. A better stress transfer, less interfacial breaking, less fiber–matrix slippage, and more fiber breaking could explain the brittle fracture. SEM characterization of the fractured surface shows that the fibers are more or less covered with remaining matrix, a qualitative indication of a larger interfacial strength.[13]

The grafting level of the different PP adhesion promoters is certainly an important parameter to consider. As already stated, a higher grafting level can induce more interfacial coupling reactions. The high reactivity of MAh can also explain the better properties generally obtained with maleated PP. Also, less viscous additives are thought to migrate more easily to the fiber–matrix interface. The mechanical properties show that the order of efficiency of the grafted PP is the same for both types of sized fibers (TSF and PSF). However, in the absence of sizing (PF), the most efficient grafted PPs are the ones of low viscosity. PP-*g*-MAl is the most efficient adhesion promoter observed in this study.

Figure 13 shows the cumulative fiber length distributions for composites containing 20 wt % TSF and either pure PP or 15% PP-*g*-MAl. It is interesting to note that both curves show similar distributions: the curves are almost parallel. The initial fiber length was 4.7 mm. After melt impregnation and injection molding, the average value ($d_{50}$) of the fiber length distribution dropped to 0.59 mm with a standard deviation (SD) of 0.42 mm for the pure PP matrix composite and to $d_{50}$ = 0.51 mm (SD = 0.37 mm) for the sample containing 15% PP-*g*-MAl. A slightly inferior value for the matrix containing PP-*g*-MAl is observed compared to that of the pure PP matrix composite. This can be explained by the increased interactions between the fibers and the PP melt containing PP-*g*-MAl. Stronger interactions between polar fibers and maleated PP are expected to promote stress transfer during melt impregnation, leading to more fiber breakage. Almost identical fiber length distributions suggest that the improvement reported for the mechanical properties of the composites is mainly due to the enhancement of the adhesion or interfacial interactions between the fibers and matrix and not to a better length to diameter ratio of the fibers.

It is difficult to compare composites of commercial and pyrolyzed fibers on the basis of their mechanical properties. Fiber attrition for composites with PF and PSF after injection molding was characterized, and the results are reported in Table V. Figures 14 and 15 show the cumulative fiber length distributions for composites containing 20 wt % of PF and PSF, respectively, and either pure PP or 15% PP-*g*-MAl. The smaller values of the fragment length can be explained by the pyrolysis of the fibers. Glass fiber pyrolysis weakens the fibers and removes all protecting layers from their surface. Consequently, feeding pyrolyzed fibers to a twin-screw extruder creates

**Table V Characterization of Fiber Attrition for Pure PP and 15% PP-*g*-MAl/85% PP Composites with Thermoplastic Sized Fibers, Pyrolyzed Fibers, and Pyrolyzed/A-1100 Sized Fibers**

| Matrix | Thermoplastic Sizing Attrition (mm) | Pyrolyzed Fibers Attrition (mm) | Pyrolyzed/A-1100 Sized Attrition (mm) |
|---|---|---|---|
| Pure PP | 0.59 ± 0.42 | 0.18 ± 0.12 | 0.20 ± 0.14 |
| 15% PP-*g*-MAl | 0.51 ± 0.37 | 0.15 ± 0.11 | 0.17 ± 0.13 |

more fiber attrition than the use of commercially sized fibers. The aspect ratio of the fibers after injection molding of the composites is an important parameter in the consideration of the mechanical performance of the specimens. For PF and PSF the attrition is therefore more important than for composites made from nonpyrolyzed commercial fibers. For this reason the mechanical properties of composites made of pyrolyzed fibers are lower than those made of commercial fibers. Nevertheless, the comparison of pure PP composites to 15% PP-*g*-MAl/PP composites indicates that in all cases the composites containing 15% grafted resin show shorter fiber fragments for both PF and PSF systems, which was previously observed for the TSF composites. The increased interactions between the fibers and the PP melt containing maleated PP is probably responsible for more fiber attrition.

## CONCLUSION

The objective of this work was to understand the parameters regulating mechanical and interfacial properties using grafted PP and a silane coupling agent as adhesion promoters. DSC showed that the addition of grafted PP increases the crystallization temperatures and the increase is more important in the presence of glass fibers. Samples containing PP-*g*-AA bearing long AA branching showed an increased secondary crystallization temperature interval, smaller crystalline morphology, and non-well-defined crystalline entities compared to the net spherulitic structures of the pure PP composite. Considering the mechanical performance improvement, PP-*g*-AA is less efficient than PP-*g*-MAh, probably because of its crystalline structure. Samples containing both PP-*g*-MA showed almost identical crystalline morphology compared to the pure PP matrix composite. PP-*g*-MAl induced better mechanical properties than PP-*g*-MAh, because of its higher level of grafting.

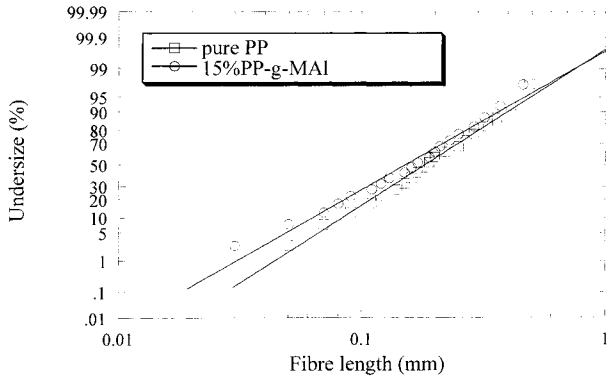


**Figure 14** Cumulative fiber length distribution for 20 wt % PF/PP composites.

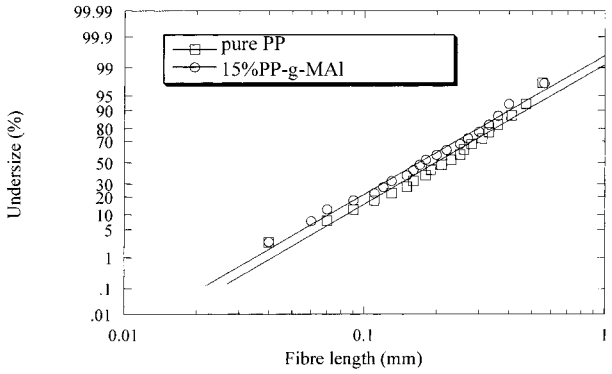


**Figure 15** Cumulative fiber length distribution for 20 wt % PSF/PP composites.

The results of the fragmentation tests on SFCs showed that the most efficient adhesion promoter was the PP-*g*-MAl, which was expected from the mechanical characterization. However, the PP-*g*-AA SFC was characterized by a smaller $l_c$ than the PP-*g*-MAh SFC. Despite the good interfacial strength, the morphology of composites containing PP-*g*-AA did not perform as well as maleated PP in improving the mechanical properties of PP composites. The results of such SFC tests have to be considered with great care until more information on the interfacial strength and its relative importance are made available.

In summary, this work shows that the interface between the matrix and fibers of composites is one of the main parameters controlling the mechanical properties of composites. The results showed that if the addition of an adhesion promoter might be necessary, the level of grafting and to a lesser extent the migration of the additive play important roles in the enhancement of the mechanical properties of the composite. Finally, appropriate sizing can promote the adhesion of the matrix to the fibers in two ways: by physical interactions and by chemical reactions between the substrates.

## REFERENCES

1. Thomason, J. L.; van Rooyen, A. A. J Mater Sci 1992, 27, 889.

2. Thomason, J. L.; van Rooyen, A. A. J Mater Sci 1992, 27, 897.
3. Denault, J. Compos Interface 1994, 2, 275.
4. Wagner, H. D.; Lustiger, A.; Marzinsky, C. N.; Mueller, M. R. R. Compos Sci Technol 1993, 48, 181.
5. Sova, M. J Appl Polym Sci 1989, 38, 511.
6. Gupta, V. B.; Mittal, R. K.; Sharma, P. K.; Menning, G.; Wolters, J. Polym Compos 1989, 10, 16.
7. Folkes, M. J.; Hardwick, S. T. J Mater Sci 1990, 25, 2598.
8. Vu-Khanh, T.; Sanschagrin, B.; Fisa, B. Polym Compos 1985, 6, 249.
9. Folkes, M. J.; Hardwick, S. T. J Mater Sci Lett 1984, 3, 1071.
10. Varga, J.; Karger-Kocsis, J. J Mater Sci Lett 1994, 13, 1069.
11. Denault, J.; Vu-Khanh, T.; Tailor, D.; Low, A. In Proceedings of SPE ANTEC '92; 1992. p 788.
12. Karian, H. G.; Wagner, H. R. In Proceedings of SPE ANTEC '93; 1993. p 3449.
13. Rijsdijk, H. A.; Contant, M.; Peijs, A. A. J. M. Compos Sci Technol 1993, 48, 161.
14. van den Oever, M. J. A.; Peijs, T. Adv Compos Lett 1994, 3, 177.
15. Tancrez, J. P.; Riestch, F.; Pabiot, J. Eur Polym J 1994, 30, 789.
16. Tancrez, J. P.; Riestch, F.; Pabiot, J. Eur Polym J 1994, 30, 803.
17. Tancrez, J. P.; Riestch, F.; Pabiot, J. Eur Polym J 1994, 30, 1479.
18. Karger-Kocsis, J. Compos Sci Technol 1993, 48, 273.
19. Yee, F. C.; Lam, W. C. Advances in Composites; Proceedings of the International Conference on Advanced Composite Materials; Minerals, Metals & Materials Society (TTIS): Warrendale, Pennsylvania, 1993. p 417.
20. Gérard, J.-F.; Chabert, B. Macromol Symp 1996, 108, 137.
21. Cheng, T. H.; Jones, F. R.; Wang, D. Compos Sci Technol 1993, 48, 89.
22. Ahlstrom, C.; Rouby, D.; Daoust, J.; Vu-Khanh, T.; Gerard, J. F. JNC 7 Comptes-Rendus des Septièmes Journées Nationales sur les Composites, Lyon, November 6–8, 1990; p 39.
23. Hoeker, F.; Karger-Kocsis, J. Composites 1994, 25, 729.
24. Kelly, A.; Tyson, W. R. J Mech Phys Solids 1965, 13, 329.
25. Champagne, M. F.; Roux, C.; Denault, J. Composites '96 and Oriented Polymers Symposium, Conference Proceedings, Boucherville, Canada, October 9–11, 1996; p 302.
26. Desaeger, M.; Wevers, M.; Verpoest, I. ICCM/9 Ceramic Matrix Composites and Other Systems, Conference Proceedings, Madrid, July 12–16, 1993; Vol. 2, p 732.
27. Herrera-Franco, P. J.; Drzal, L. T. Composites 1992, 23, 2.
28. Narkis, M.; Chen, E. J. H.; Pipes, R. B. Polym Compos 1988, 9, 245.
29. Ide, F.; Hasegawa, A. J Appl Polym Sci 1974, 18, 963.
30. Asthana, H.; Jayaraman, K. ACS Meeting Rubber Division, Conference Proceedings, Nashville, TN, Sept 29–Oct 2, 1998, paper 61.
31. Karger-Kocsis, J. Polypropylene: Structure, Blends and Composites, Volume 3, Composites; Chapman & Hall: London, 1995.
32. Cebe, P. Polym Compos 1988, 9, 271.